JOURNAL OF Materials CHEMISTRY

Moderate hydrothermal synthesis of layered caesium titanate

Naruhiko Masaki,* Satoshi Uchida and Tsugio Sato

Institute of Multidisciplinary Research for Advanced Materials, Tohoku University, Katahira Aoba-ku, Sendai 980-8577, Japan. Tel: +81-22-217-5599; Fax: +81-22-217-5599; E-mail: masaki@kuroppe.icrs.tohoku.ac.jp

Received 23rd July 2001, Accepted 25th October 2001
First published as an Advance Article on the web 12th December 2001

The hydrothermal oxidation of Ti metal powder was performed in *ca.* 0.1–55 mol $(kg\ H_2O)^{-1}$ caesium hydroxide solutions in the range 150 to 350 °C. Lepidocrocite-type caesium titanate ($Cs_xTi_{2-x/4}\square_{x/4}O_4$) ($\square$ = vacancy) has been successfully obtained as a single phase even at the low temperature of 150 °C. Resultant caesium titanate forms plate-like particles with an average size of *ca.* 0.59 μm in length. At higher caesium hydroxide concentrations and reaction temperatures, amorphous products which transform into $Cs_xTi_{2-x/4}\square_{x/4}O_4$ by calcination above 750 °C are obtained. A formation diagram of products in the Ti–CsOH–H_2O system has been constructed for a CsOH concentration range of 0.1–55 mol $(kg\ H_2O)^{-1}$ and for the temperature range 150–350 °C.

Introduction

It is well known that various alkali titanates represented by the chemical formula $A_2O{\cdot}nTiO_2$ (A = alkali metal ion, $n \approx 2-9$) have their own crystal structures of layered- or tunnel-type. Since those titanates show excellent ion exchange ability,[1–5] they have been applied to ion exchange reactions for the fixing of radioactive metal ions,[6–8] as starting materials for the intercalation of organic compounds,[9–13] or for the fabrication of porous materials.[14–18] Another particularly interesting property of these compounds is their photocatalytic activities.[18–25]

As shown in Fig. 1, lepidocrocite-type caesium titanate has a unique layer structure which is flat along the *c*-axis.[26–28] As a consequence of this structure, interlayer protons of the protonated lepidocrocite-type titanate are readily exchanged by other alkali metal ions.[29,30] In recent years, it has been reported that protonated lepidocrocite-type titanate can be easily exfoliated into single layers by the intercalation of bulky organic amines to fabricate plate-like particles of titania and thin films of protonic titanate.[24,31–33] The titania films are also attractive because of their application to dye-sensitized TiO_2 solar cells.[34–37]

In order to improve functional properties such as photocatalytic activity or ion exchange ability, it is highly desirable to be able to control the particle size and morphology of the titanates. From this point of view, hydrothermal synthesis is a suitable method. However, the formation of caesium titanate under hydrothermal conditions has not yet been reported. Meanwhile we have reported that various potassium titanates are produced under hydrothermal conditions using metallic Ti powder as a raw material within a short reaction time and without a second phase product.[38,39] In this study, therefore, the hydrothermal reactions of Ti powder in caesium hydroxide solutions at 150 to 350 °C have been investigated for the first time.

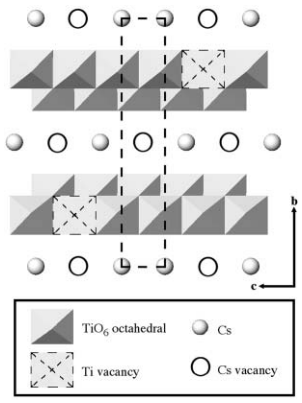

Fig. 1 Polyhedral representation of the crystal structure for $Cs_xTi_{2-x/4}\square_{x/4}O_4$ ($x = 0.62$; $\square$, vacancy) viewed down the *a* axis. Broken lines encircle the body-centered unit cell.

Experimental section

Reagents and materials

All chemicals used were of reagent grade. Ti powder (Wako Pure Chemical Industries, Ltd.) used as a starting material was of min. 95% purity with particles of < 45 μm in diameter.

Hydrothermal oxidation of titanium powder

Initially, 1.0 g $CsOH{\cdot}H_2O$ (Nacalai tesque, Inc.), 0.1 g Ti powder and sufficient deionized water to achieve the desired CsOH concentration were put into an autoclave of 100 cm^3 internal volume, constructed from SUS 316 type stainless steel. To prevent further corrosion of the steel, a polytetrafluoroethylene (Teflon®) cup and a Ni beaker were placed inside the autoclave below and above 300 °C, respectively. After sealing, the autoclave was placed in an electric furnace at the desired temperature for 2 h. During the reaction period, the autoclave was kept at an autogeneous saturation vapor pressure of the solution without stirring. The product was separated from the solution by centrifuge, then rinsed with methanol and finally dried in an oven at 105 °C for 12 h.

Characterization

Products were identified by X-ray powder diffraction (Shimadzu diffract meter XD-D1) using graphite-monochromatized Cu Kα radiation. Chemical analysis was carried out by ICP-AES (Perkin-Elmer Optima 3300) and AAS (Shimadzu AA-6500S) after dissolving the sample in *aqua regia*. Thermal analysis of products was also performed in air with a heating rate of 10 °C min^{-1} using a Rigaku TAS-200 thermogravimetric analyzer. The morphology of products was observed by SEM (Hitachi S-430 and S-900). The specific surface area was determined by nitrogen adsorption using a Quantachrome NOVA1000-TS.

Results and discussion

Formation diagram of the Ti–CsOH–H_2O system

A series of experiments on the Ti–CsOH–H_2O system was carried out for the CsOH concentration range 0.1–55 mol (kg H_2O)$^{-1}$ and at temperatures from 150 to 350 °C. Typical XRD patterns of products at 250 °C together with a formation diagram of the Ti–CsOH–H_2O system are shown in Figs. 2 and 3, respectively.

In Fig. 2 formation of lepidocrocite-type caesium titanate ($Cs_xTi_{2-x/4}\square_{x/4}O_4$) was observed for a CsOH solution of 1 mol (kg H_2O)$^{-1}$; however, the sample mainly consisted of unreacted titanium powder. Single phase $Cs_xTi_{2-x/4}\square_{x/4}O_4$ was successfully obtained for CsOH solutions of 5 to 10 mol (kg H_2O)$^{-1}$. At CsOH concentrations above 20 mol (kg H_2O)$^{-1}$, the amorphous phase was formed. From the formation diagram, Fig. 3, there is a tendency to form the amorphous compound at lower CsOH concentrations such as 10 mol (kg H_2O)$^{-1}$ above 300 °C. This means that the region of CsOH concentration where $Cs_xTi_{2-x/4}\square_{x/4}O_4$ is stable narrows with increasing reaction temperature.

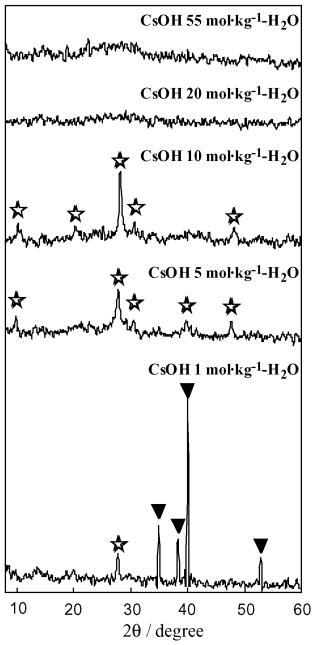

Fig. 2 XRD patterns of products after hydrothermal treatment in CsOH solution for 2 h at 250 °C. ▼, Ti; ☆, $Cs_xTi_{2-x/4}\square_{x/4}O_4$. (Set up condition: Cs : Ti = 2.9.)

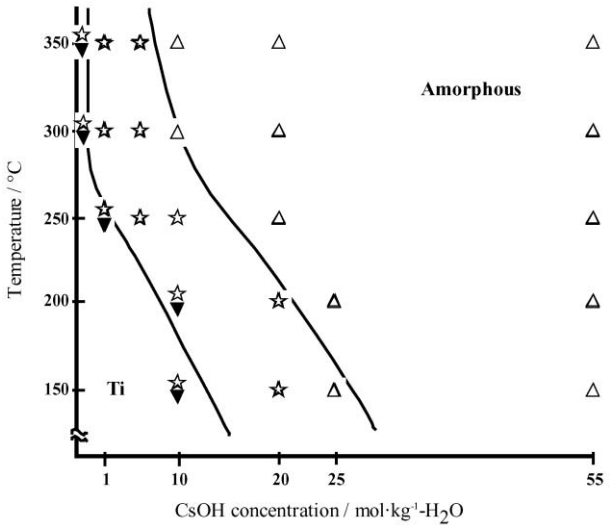

Fig. 3 Formation diagram of products in the Ti–CsOH–H_2O system at various temperatures for 2 h. ▼, Ti; ☆, $Cs_xTi_{2-x/4}\square_{x/4}O_4$; △, amorphous.

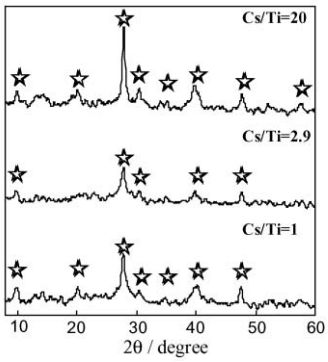

Fig. 4 XRD patterns of products after hydrothermal treatment for 2 h at 250 °C. ☆, $Cs_xTi_{2-x/4}\square_{x/4}O_4$. (Set up condition: 5 mol (kg H_2O)$^{-1}$ CsOH solution.)

In this series of experiments, only $Cs_xTi_{2-x/4}\square_{x/4}O_4$ was found as a crystallized phase. It can be considered that this result is affected by the Cs : Ti molar ratio fixed at 2.9. In view of this, therefore, the effect of the Cs : Ti molar ratio at 5 mol (kg H_2O)$^{-1}$ CsOH was examined at 250 °C.

The results are shown in Fig. 4. All products were identified by XRD as $Cs_xTi_{2-x/4}\square_{x/4}O_4$ and no effect of varying the Cs : Ti molar ratio on the resultant compound could be observed.

Chemical composition and morphology of products

Table 1 shows the results of chemical analysis of the products. The caesium molar content, x, of $Cs_xTi_{2-x/4}\square_{x/4}O_4$ obtained at 5 mol (kg H_2O)$^{-1}$ for CsOH and 250 °C was 0.68. It is certain that the lepidocrocite-type structure of $Cs_xTi_{2-x/4}\square_{x/4}O_4$ sample was maintained until x could vary from 0.58 to 0.90.[28] From this result, it can be considered that the amorphous phase tends to form at relatively higher CsOH concentration or higher reaction temperature because such a condition exceeds the stability region of the lepidocrocite phase.

The morphology of the product was observed by SEM. Scanning electron micrographs of typical products are shown in Fig. 5. The $Cs_xTi_{2-x/4}\square_{x/4}O_4$ sample formed at 250 °C for the 10 mol (kg H_2O)$^{-1}$ CsOH solution consisted of an aggregate of fine particles of average size 0.59 μm [Fig. 5(a)]. Therefore, high resolution SEM observation was also performed for this sample [Fig. 5(b)]. This micrograph reveals that the initially formed small plate particles aggregate with size about 0.2 μm, and that the particles seen in Fig. 5(a), with an average size of about 0.59 μm, are aggregates of these secondary particles. The specific surface area (SSA) of this sample determined by three points of the B.E.T. method is 77.9 m^2 g^{-1}. The SSA is larger than that of the titanate synthesized by the conventional solid state reaction (*ca.* 1–3 m^2 g^{-1}) and this suggests a unique character of this synthesis method. The amorphous sample formed at 55 mol (kg H_2O)$^{-1}$ CsOH and

Table 1 Chemical analyses of the products by ICP-AES and AAS

Sample	Content/wt% Cs	Content/wt% Ti	Calc. x for $Cs_xTi_{2-x/4}\square_{x/4}O_4$
$Cs_xTi_{2-x/4}\square_{x/4}O_4$ (calc.)[a]	33.5 ~ 44.5	31.6 ~ 38.6	*ca.* 0.58–0.90
$Cs_xTi_{2-x/4}\square_{x/4}O_4$[b]	38.7	37.4	0.68
$Cs_xTi_{2-x/4}\square_{x/4}O_4$[c]	51.7	29.3	1.09

[a]Calculated from ref. 28. [b]Obtained at 5 mol (kg H_2O)$^{-1}$ CsOH and 250 °C. [c]Obtained at 55 mol (kg H_2O)$^{-1}$ CsOH and 350 °C.

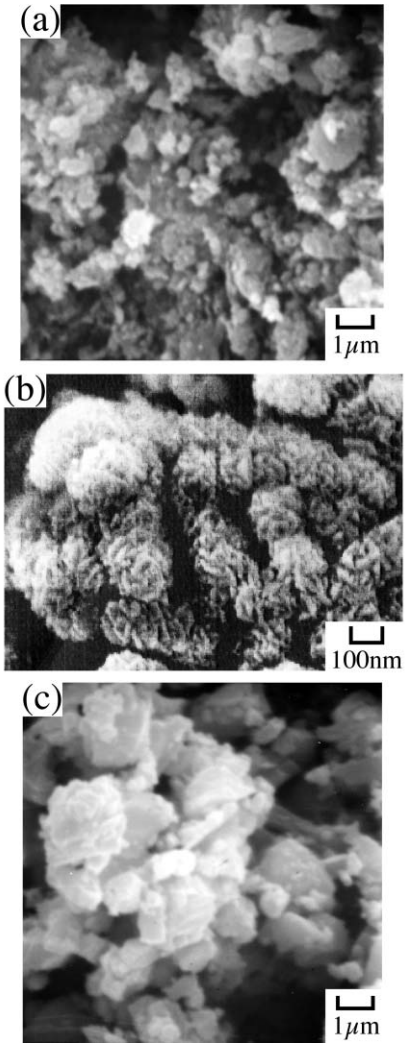

Fig. 5 SEM photographs of products: (a) $Cs_xTi_{2-x/4}\square_{x/4}O_4$ formed at 10 mol (kg H_2O)$^{-1}$ CsOH and 250 °C; (b) high resolution image of (a); (c) amorphous compound formed at 55 mol (kg H_2O)$^{-1}$ CsOH and 350 °C.

350 °C consists of plate-like particles with average size of 0.93 μm [Fig. 5(c)]. It can be seen that the amorphous sample is larger than $Cs_xTi_{2-x/4}\square_{x/4}O_4$ in particle size and is more uniform. It is supposed that these differences are due to the severe synthetic conditions of the amorphous sample where the growth of particles by a dissolution–reprecipitation mechanism may be relatively accelerated.

Thermal properties of products

The results of TG–DTA analysis of typical products are shown in Fig. 6. The $Cs_xTi_{2-x/4}\square_{x/4}O_4$ sample obtained for the 10 mol (kg H_2O)$^{-1}$ CsOH solution at 250 °C shows weight losses up to 200 °C and above 1000 °C. The former is due to the desorption of remaining water and this was confirmed by IR spectroscopy. The latter is possibly caused by the vaporization of Cs_2O. The endothermic peak corresponding to the melting of $Cs_xTi_{2-x/4}\square_{x/4}O_4$ was also observed at around 1100 °C which agrees with the literature.[26] The results of amorphous sample obtained at 20 mol (kg H_2O)$^{-1}$ CsOH and 250 °C also show two stage weight losses and the endothermic peak. Additionally, two exothermic peaks at 405 and 563 °C, which are due to rearrangement resulting from crystallization, are observed. This is the most distinct difference between the amorphous and crystalline samples.

To understand thermal stability, the samples were heated in air using an electric furnace at various temperatures for 1 h.

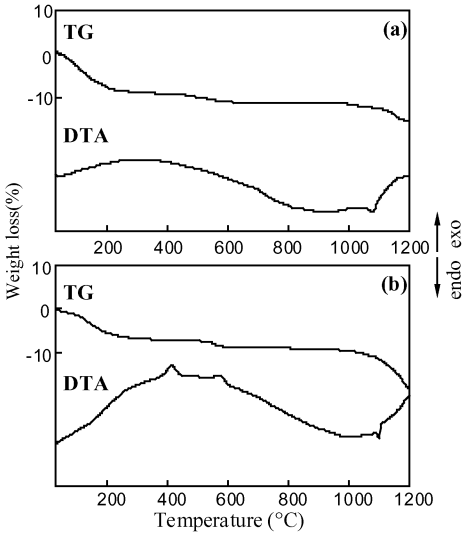

Fig. 6 TG–DTA curves of products: (a) $Cs_xTi_{2-x/4}\square_{x/4}O_4$ formed at 10 mol (kg H_2O)$^{-1}$ CsOH and 250 °C; (b) amorphous compound formed at 55 mol (kg H_2O)$^{-1}$ CsOH and 350 °C.

Fig. 7 shows the XRD patterns of the samples after heat treatment. By heat treatment at 750 °C, the crystallinity of $Cs_xTi_{2-x/4}\square_{x/4}O_4$ is improved. Since the final product is rutile, it is supposed that the weight loss above 1000 °C is due to the decomposition of $Cs_xTi_{2-x/4}\square_{x/4}O_4$ to form TiO_2. The XRD patterns of samples after heat treatment of the amorphous sample formed at 10 mol (kg H_2O)$^{-1}$ CsOH and 350 °C are also shown in Fig. 7(b). Crystallization of the

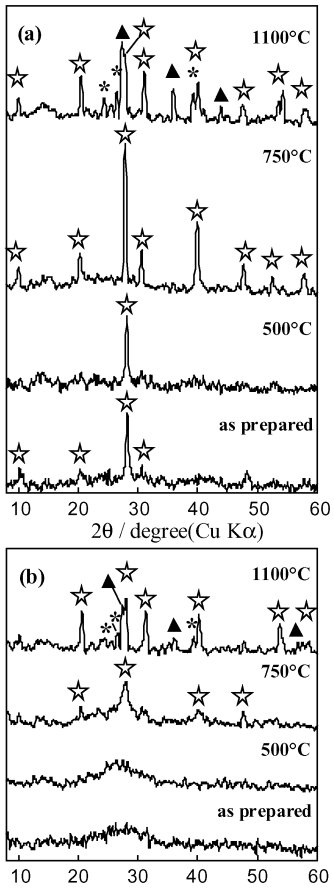

Fig. 7 XRD patterns of products after heat treatment at various temperature for 1 h: (a) $Cs_xTi_{2-x/4}\square_{x/4}O_4$ formed at 10 mol (kg H_2O)$^{-1}$ CsOH and 250 °C; (b) amorphous compound formed at 10 mol (kg H_2O)$^{-1}$ CsOH and 350 °C. ☆, $Cs_xTi_{2-x/4}\square_{x/4}O_4$; ▲, TiO_2 (rutile); *, Cs_2CO_3.

amorphous phase into $Cs_xTi_{2-x/4}\square_{x/4}O_4$ was observed above 750 °C and the decomposition of resultant $Cs_xTi_{2-x/4}\square_{x/4}O_4$ to TiO_2 could be also identified at 1150 °C.

Conclusion

From the results of tests described above, the following conclusions may be drawn:

1. A formation diagram of products in the Ti–CsOH–H_2O system has been constructed at the region of CsOH concentration from 0.1 to 55 mol $(kg\ H_2O)^{-1}$ and at temperatures in the range 150–350 °C.

2. A single phase of $Cs_xTi_{2-x/4}\square_{x/4}O_4$ is formed at CsOH concentration in the range 1–25 mol $(kg\ H_2O)^{-1}$ and at temperatures from 150 to 350 °C.

3. $Cs_xTi_{2-x/4}\square_{x/4}O_4$ formed at 10 mol $(kg\ H_2O)^{-1}$ CsOH and 250 °C consists of an aggregate of particles of size *ca.* 0.2 μm.

4. $Cs_xTi_{2-x/4}\square_{x/4}O_4$ is expected to exhibit an improved ability as an ion exchanger since this product shows a large SSA of 77.9 $m^2\ g^{-1}$.

References

1 R. Marchand, L. Brohan, R. M'Bedi and M. Tournoux, *Rev. Chim. Miner.*, 1984, **21**, 476.
2 T. Sasaki, M. Watanabe, Y. Komatsu and Y. Fujiki, *Inorg. Chem.*, 1985, **24**, 2265.
3 H. Izawa, S. Kikkawa and M. Koizumi, *J. Solid State Chem.*, 1985, **60**, 264.
4 H. Izawa, S. Kikkawa and M. Koizumi, *J. Phys. Chem.*, 1982, **86**, 5023.
5 T. Sasaki, Y. Komatsu and Y. Fujiki, *Chem. Mater.*, 1992, **4**, 894.
6 Y. Fujiki, Y. Komatsu and N. Ohta, *Chem. Lett.*, 1980, 1023.
7 T. Sasaki, Y. Komatsu and Y. Fujiki, *Chem. Lett.*, 1981, 957.
8 E. A. Behrens, P. Sylvester and A. Clearfield, *Environ. Sci. Technol.*, 1998, **32**, 101.
9 T. Sasaki, F. Izumi and M. Watanabe, *Chem. Mater.*, 1996, **8**, 777.
10 H. Izawa, S. Kikkawa and M. Koizumi, *Polyhedron*, 1983, **2**, 741.
11 H. Izawa, S. Kikkawa and M. Koizumi, *J. Solid State Chem.*, 1987, **69**, 336.
12 H. Miyata, Y. Sugahara, K. Kuroda and C. Kato, *J. Chem. Soc., Faraday Trans. 1*, 1988, **84**, 2677.
13 T. Nakato, K. Kusunoki, K. Yoshizawa, K. Kuroda and M. Kaneko, *J. Phys. Chem.*, 1995, **99**, 17 896.
14 S. Cheng and T-C. Wang, *Inorg. Chem.*, 1989, **28**, 1283.
15 J. N. Kondo, S. Shibata, Y. Ebina, K. Domen and A. Tanaka, *J. Phys. Chem.*, 1995, **99**, 16 043.
16 M. Machida, J. Yabunaka, H. Taniguchi and T. Kijima, *Stud. Surf. Sci. Catal.*, 1998, **118**, 95.
17 F. Kooli, T. Sasaki and M. Watanabe, *Langmuir*, 1999, **15**, 1090.
18 M. Machida, X. W. Ma, H. Taniguchi, J. Yabunaka and T. Kijima, *J. Mol. Catal. A: Chem.*, 2000, **155**, 131.
19 Y. Inoue, T. Kubokawa and K. Sato, *J. Chem. Soc., Chem. Commun.*, 1990, 1298.
20 Y. Inoue, T. Kubokawa and K. Sato, *J. Phys. Chem.*, 1991, **95**, 4059.
21 Y. I. Kim, S. J. Atherton, E. S. Brigham and T. E. Mallouk, *J. Phys. Chem.*, 1993, **97**, 11 802.
22 M. Kohno, S. Ogura, K. Sato and Y. Inoue, *Stud. Surf. Sci. Catal.*, 1996, **101**, 143.
23 T. Sato, Y. Yamamoto, Y. Fujishiro and S. Uchida, *J. Chem. Soc., Faraday Trans.*, 1996, **92**, 5089.
24 A. Kudo and T. Kondo, *J. Mater. Chem.*, 1997, **7**, 777.
25 T. Sasaki, S. Nakano, S. Yamauchi and M. Watanabe, *Chem. Mater.*, 1997, **9**, 602.
26 I. E. Grey, I. C. Madsen, J. A. Watts, L. A. Bursill and J. Kwiatkowska, *J. Solid State Chem.*, 1985, **58**, 350.
27 I. E. Grey, I. C. Madsen and J. A. Watts, *J. Solid State Chem.*, 1987, **66**, 7.
28 M. Hervieu and B. Raveau, *Rev. Chim. Miner.*, 1981, **18**, 642.
29 T. Sasaki, Y. Komatsu and Y. Fujiki, *J. Chem. Soc., Chem. Commun.*, 1991, 817.
30 T. Sasaki, M. Watanabe, Y. Michiue, Y. Komatsu, F. Izumi and S. Takenouchi, *Chem. Mater.*, 1995, **7**, 1001.
31 T. Sasaki, M. Watanabe, H. Hashizume, H. Yamada and H. Nakazawa, *J. Am. Chem. Soc.*, 1996, **118**, 8329.
32 T. Sasaki, M. Watanabe, H. Hashizume, H. Yamada and H. Nakazawa, *Chem. Commun.*, 1996, 229.
33 R. Abe, K. Shinohara, A. Tanaka, M. Hara, J. N. Kondo and K. Domen, *Chem. Mater.*, 1998, **10**, 329.
34 B. O'Regan and M. Gräzel, *Nature*, 1991, **353**, 737.
35 A. Shiga, A. Tsujiko, T. Ide, S. Yae and Y. Nakato, *J. Phys. Chem.*, 1998, **102**, 6049.
36 J. Weidmann, Th. Dittrich, E. Konstantinova, I. Lauermann, I. Uhlendorf and F. Koch, *Sol. Energy Mater. Sol. Cells*, 1999, **56**, 153.
37 A. F. Nogueira and M.-A. D. Paoli, *J. Mater. Sci.*, 2000, **61**, 135.
38 N. Masaki, S. Uchida, H. Yamane and T. Sato, *J. Mater. Sci.*, 2000, **35**, 3307.
39 S. Uchida, N. Masaki, H. Yamane and T. Sato, *High Pressure Res.*, 2001, **21**, in press.